Supplementary Information of

Preparation of organophosphorus modified SBA-15 for effective adsorption of Congo red and Reactive red 2

Fan Zhang [a, b], Chuting Yang [b], Yi Li [b], Min Chen [a, c], Sheng Hu [b], Haiming Cheng *[a, c]

a. National Engineering Laboratory for Clean Technology of Leather Manufacture, Sichuan University, Chengdu 610065, Sichuan, China

b. Institute of Nuclear Physics and Chemistry, China Academy of Engineering physics, Mianyang 621900, Sichuan, China

c. The Key Laboratory of Leather Chemistry and Engineering of Ministry of Education, Sichuan University, Chengdu 610065, China

Table of Contents

Nomenclature	
C_0	Initial dye concentration of solution (mg/L)
C_e	Equilibrium concentration of the dye in solution (mg/L)
R	Dye removal percentage (%)
m	Adsorbent weight (mg)
V	Volume of solutions (mL)
q_e	Amount of dye adsorbed at equilibrium
q_t	Amount of dye adsorbed at time t
q_m	The maximum adsorption capacity for monolayer adsorption (mg/g)
K_L	Langmuir constant (L/mg)
K_F	Freundlich isotherm constant related to adsorption capacity
K_T	The maximum binding energy constant (L/mg)
B_T	Temkin constant related to the heat of adsorption
n	Freundlich isotherm constant related to adsorption intensity
R^2	Linear correlation coefficient
R_L	Dimensionless constant separation factor
k_1	Pseudo-first order rate constant (min^{-1})
k_2	Pseudo-second order rate constant (g/mg·min)
k_{id}	Intra-particle diffusion rate constant ($mg/g \cdot min^{1/2}$)
t	Contact time (min)
C_i	Intercept related to the thickness of the boundary layer
α	Initial sorption rate in the Elovich model (mg/g·min)
β	Constant related to the extent of surface coverage and activation energy for chemisorption in the Elovich model (g/mg)
ΔG^o	Gibbs free energy (kJ/mol)
ΔH^o	Enthalpy (kJ/mol)
ΔS^o	Entropy (J/mol·K)
K_d	Distribution coefficient (mL/g)
R	Ideal gas constant (8.314 J/mol·K)
T	Absolute temperature (K)

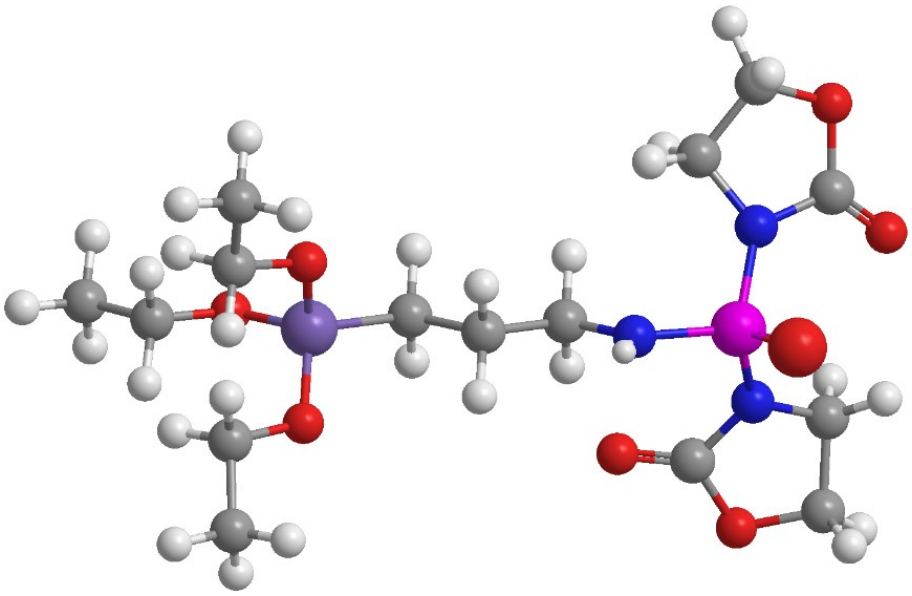

Fig. S1. The chemical structure of APTES-BOP ligand.

APTES-BOP Ligand analysis:

P,P-bis(2-oxooxazolidin-3-yl)-N-(3-(triethoxysilyl)propyl)phosphinic amide.

^{1}H NMR (600 MHz, $CDCl_3$) δ 4.47 – 4.31 (m, 4H), 4.17 (dd, *J* = 16.5, 7.1 Hz, 1H), 4.03 (td, *J* = 8.9, 1.0 Hz, 2H), 3.91 (td, *J* = 9.0, 6.8 Hz, 2H), 3.72 (dq, *J* = 69.0, 7.0 Hz, 6H), 3.07 (dq, *J* = 14.1, 7.0 Hz, 2H), 1.67 – 1.55 (m, 2H), 1.19 (dt, *J* = 10.7, 5.8 Hz, 9H), 0.68 – 0.51 (m, 2H).

^{13}C NMR (151 MHz, $CDCl_3$) δ 156.6 (d, *J* = 9.4 Hz), 63.9 (d, *J* = 8.6 Hz), 58.4 (d, *J* = 19.8 Hz), 44.5 (d, *J* = 4.0 Hz), 42.9, 29.7, 18.4 (d, *J* = 17.8 Hz), 7.47. HRMS calcd for $C_{15}H_{30}N_3O_8PSi$ (M+): 439.1540; found: 439.1542.

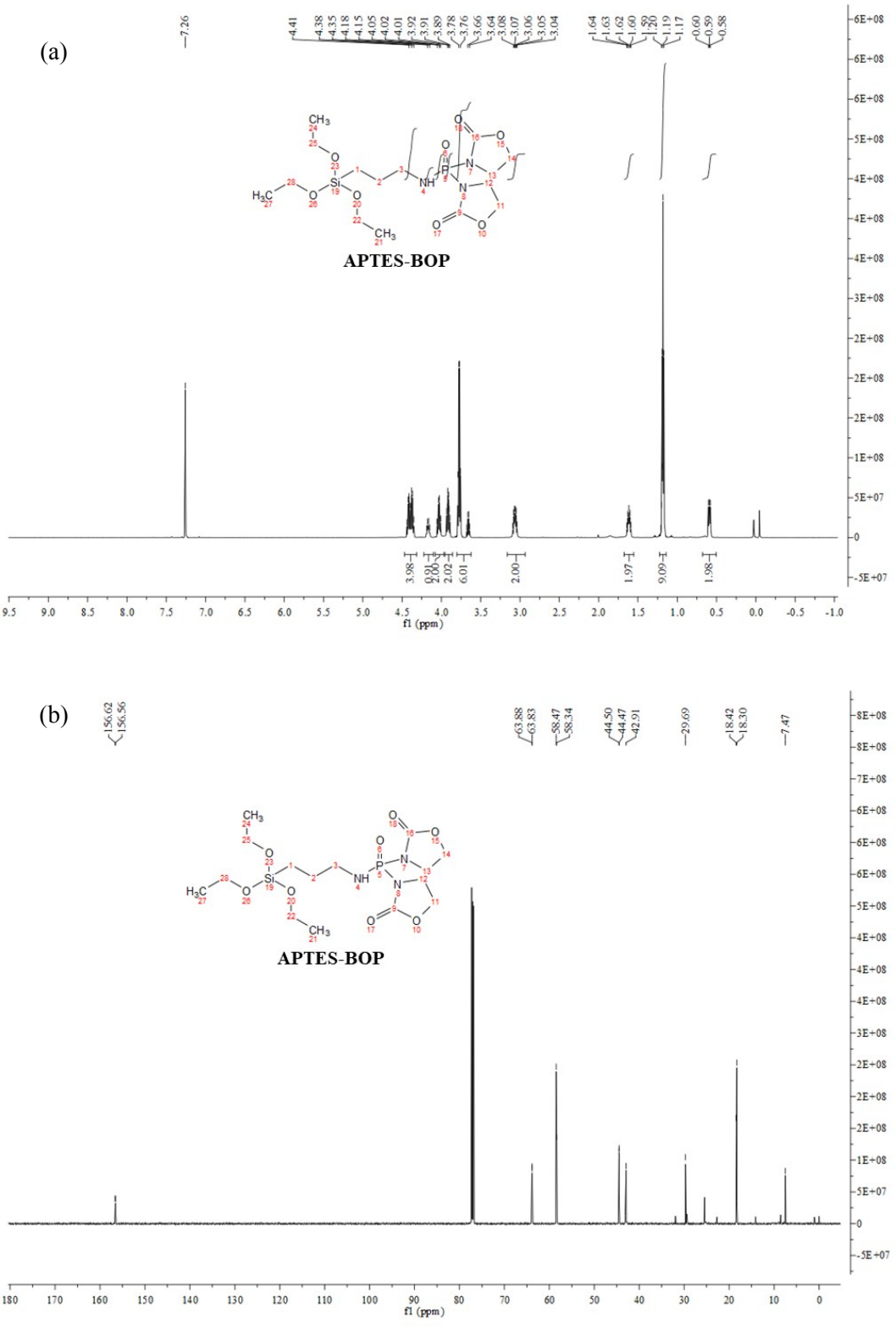

Fig. S2. (a) the ^{1}H NMR and (b) ^{13}C NMR spectra of APTES-BOP.

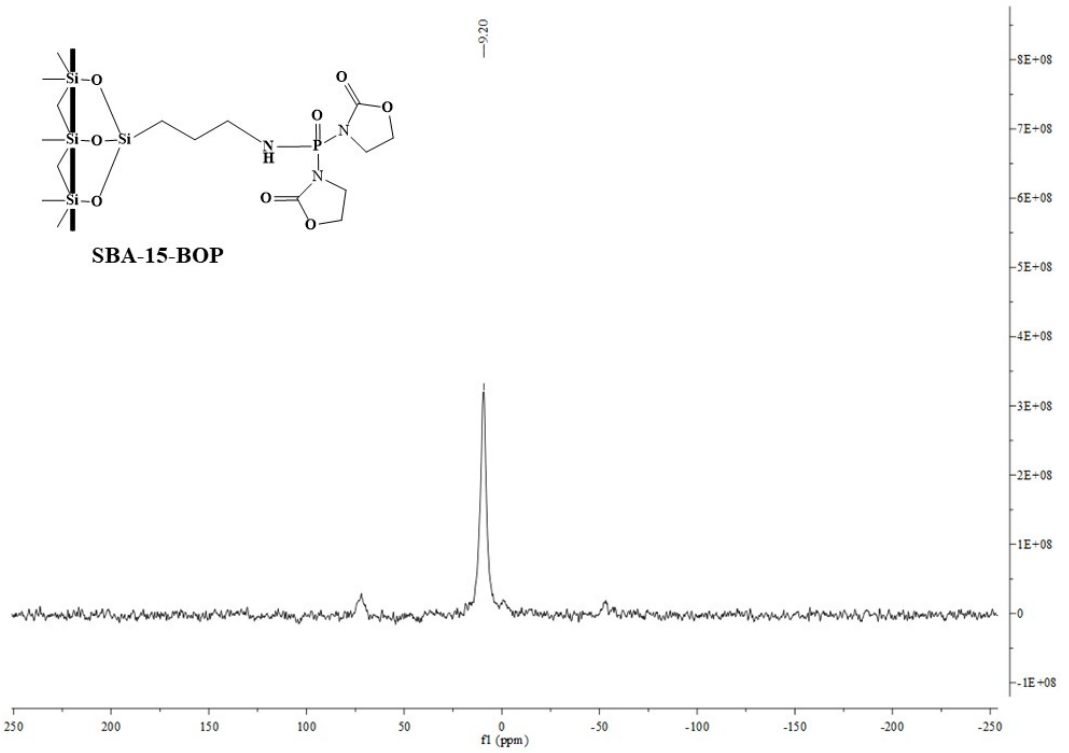

Fig. S3. Solid state ^{31}P CP-MAS NMR spectra of SBA-15-BOP.

Table S1 Molecular structure and properties of the investigated dyes

Characteristic	CR	RR2
Molecular Formula	$C_{32}H_{22}N_6Na_2O_6S_2$	$C_{19}H_{10}Cl_2N_6Na_2O_7S_2$
Commercial Name	Congo Red	Reactive Red 2
Color Index NO.	C.I. Direct Red 28	C.I. Reactive Red 2
Class	Direct Dye	Reactive Dye
Molecular Weight (g/mol)	696.66	615.33
λ_{max}	498nm	539nm
Molecular Structure	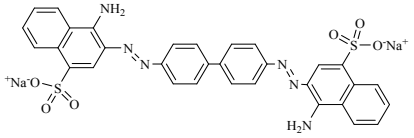	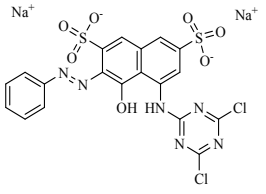

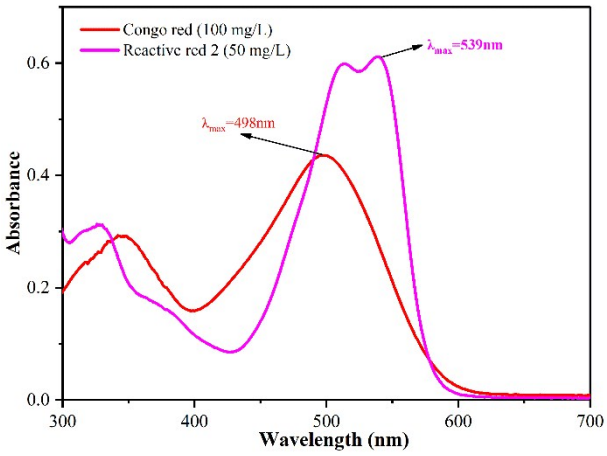

Fig. S4. The absorption spectrogram of CR and RR2. (at natural pH conditions; T = 25 ℃)

Table S2 Typical adsorption isotherms, kinetics models and thermodynamic equations have been investigated in the present work[1-3].

Model	Equation
Langmuir isotherm	$C_e / q_e = 1 / K_L q_m + C_e / q_m$ $R_L = \frac{1}{(1 + K_L C_0)}$
Freundlich isotherm	$\ln q_e = \ln K_F + \ln C_e / n$
Temkin isotherm	$q_e = B_T \ln K_T + B_T \ln C_e$
Pseudo-first-order model	$1 / q_t = 1 / (q_e t) + 1 / q_e$
Pseudo-second-order model	$t / q_t = 1 / (k_2 q_e^2) + t / q_e$
Simple Elovich model	$q_t = \frac{\ln \alpha\beta}{\beta} + \frac{\ln t}{\beta}$
Intra-particle diffusion model	$q_t = k_{id} t^{1/2} + C_i$ $K_d = \frac{C_0 - C_e}{C_e} \times \frac{V}{m}$
Thermodynamic study	$\Delta G^\circ = \Delta H^\circ - T\Delta S^\circ$ $\ln K_d = \Delta S^\circ / R - \Delta H^\circ / RT$

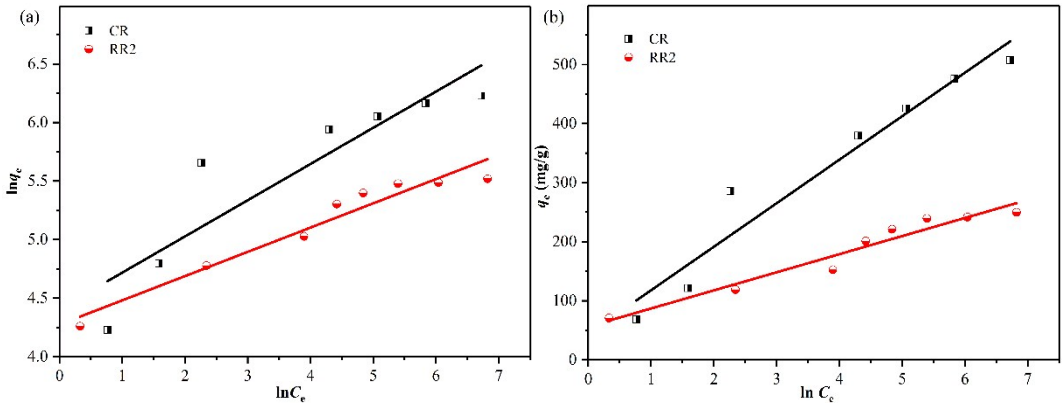

Fig. S5. The isotherms of (a) Freundlich and (b) Temkin models for dye adsorption onto SBA-15-BOP.

Table S3 Isotherm parameters for CR and RR2 adsorption on SBA-15-BOP

Isotherms	Parameters	CR	RR2
Langmuir	K_L (L/mg)	0.04467	0.05786
	q_m（mg/g）	518.1	253.8
	R^2	0.9984	0.9991
Freundlich	K_F (L/mg)	82.17	71.82
	n	3.234	4.829
	R^2	0.7984	0.9374
Temkin	K_T (L/mg)	5.308	1.724
	B_T	73.67	30.65
	R^2	0.9350	0.9400

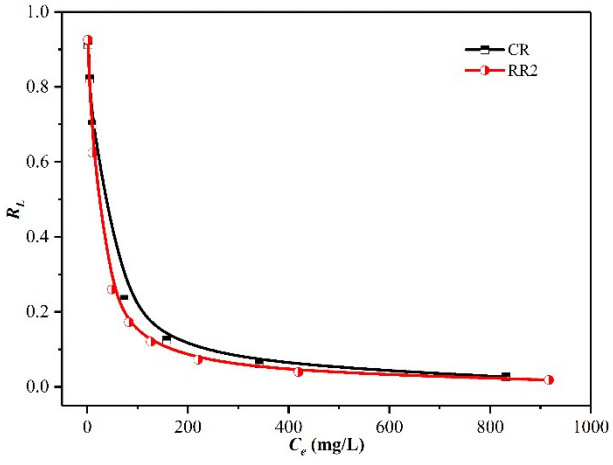

Fig. S6. The plot of R_L versus C_e.

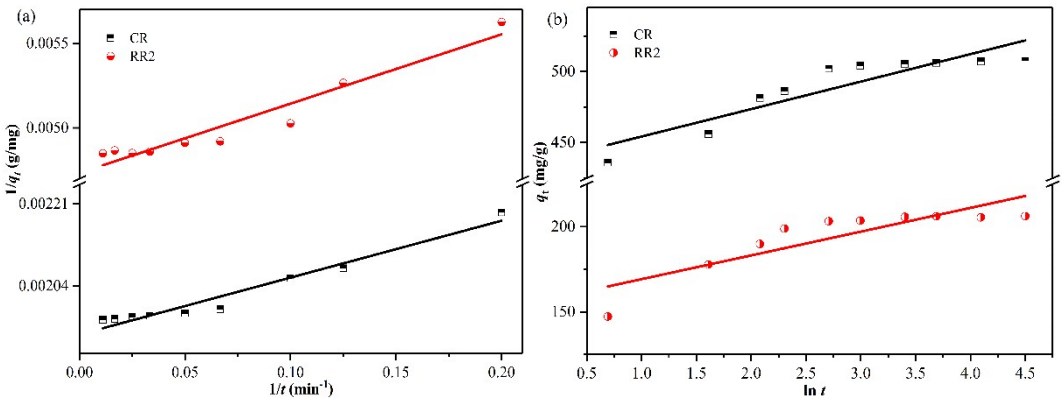

Fig. S7. (a) pseudo-first-order and (b) Elovich models for dye adsorption onto SBA-15-BOP.

Table S4 Kinetic parameters for CR and RR2 adsorption on SBA-15-BOP

Kinetic model	Parameters	CR	RR2
Pseudo-first-order	q_t (mg/g)	496.0	201.7
	k_1 (min^{-1})	1.020	0.5952
	R^2	0.9889	0.9876
Pseudo-second-order	q_t (mg/g)	507.6	206.6
	k_2 (g/mg·min)	0.009164	0.01845
	R^2	0.9999	0.9999
Elovich	α (mg/g·min)	1.12E+11	9.54E+05
	β (g/mg)	0.0517	0.0717
	R^2	0.8065	0.7146

Table S5 Intra-particle diffusion model parameters for CR and RR2 adsorption on SBA-15-BOP

Dye	C_0 (mg/L)	k_{1d} (mg/g·min$^{1/2}$)	k_{2d} (mg/g·min$^{1/2}$)	k_{3d} (mg/g·min$^{1/2}$)	C_1	C_2	C_3	$(R_1)^2$	$(R_2)^2$	$(R_3)^2$
CR	200	308.2	27.88	0.9096	0	397.0	499.8	1	0.9747	0.8172
RR2	200	111.2	19.22	0.5780	0	132.5	201.3	1	0.9399	0.8075

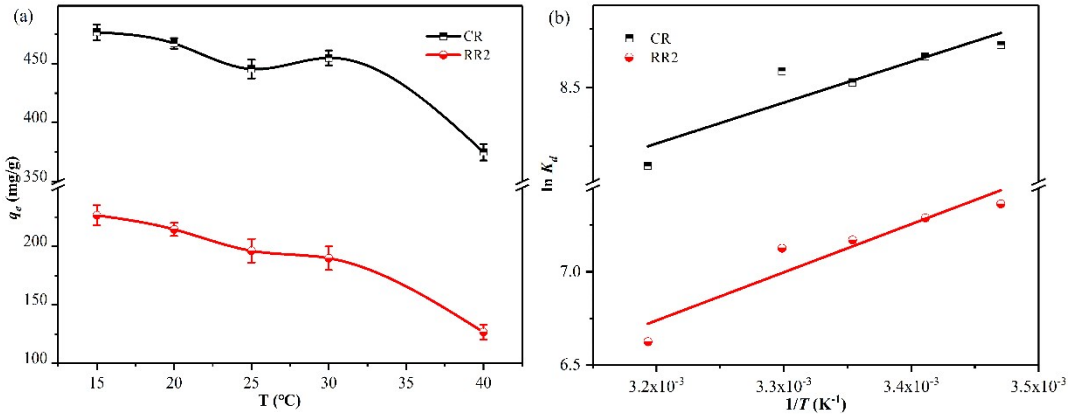

Fig. S8. (a) effect of contact time on the adsorption; (b) the plot of lnK_d versus 1/T.
(dyes concentration = 200 mg/L, V/m = 3 mL/mg, t = 60 min)

Table S6 Thermodynamic parameters for CR and RR2 adsorption on SBA-15-BOP

Dye	ΔH^o (kJ/mol)	ΔS^o (J/mol·K)	ΔG^o (kJ/mol)				
			288 K	293 K	298 K	303 K	313 K
CR	-14.43	22.52	-20.92	-21.03	-21.14	-21.26	-21.48
RR2	-21.53	-12.87	-17.82	-17.76	-17.69	-17.63	-17.50

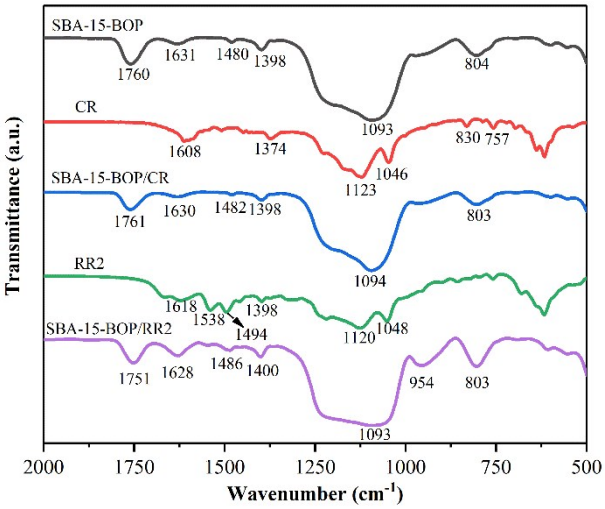

Fig. S9. FT-IR spectra of SBA-15-BOP before and after adsorbing both dyes.

References

[1] Z. Wu, H. Zhong, X. Yuan, H. Wang, L. Wang, X. Chen, G. Zeng, Y. Wu, Adsorptive removal of methylene blue by rhamnolipid-functionalized graphene oxide from wastewater, Water Res, 67 (2014) 330-344.

[2] F. Zhang, M. Chen, S. Hu, H. Cheng, Chemical treatments on the cuticle layer enhancing the uranium(VI) uptake from aqueous solution by amidoximated wool fibers, Journal of Radioanalytical and Nuclear Chemistry, 314 (2017) 1927-1937.

[3] L. Largitte, R. Pasquier, A review of the kinetics adsorption models and their application to the adsorption of lead by an activated carbon, Chemical Engineering Research and Design, 109 (2016) 495-504.